JOURNAL OF CATALYSIS 152, 204–210 (1995)

Catalytic Performance of Supported Alkali Molten Carbonate towards the Oxidative Dimerization of Methane

V. Tashjian, M. Cassir,[1] and J. Devynck

Ecole Nationale Supérieure de Chimie de Paris, Laboratoire d'Electrochimie et de Chimie Analytique (URA 216 du CNRS),
11 Rue Pierre et Marie Curie, 75231 Paris Cédex 05, France

Received March 18, 1994; September 16, 1994

Catalytic performance of Na_2CO_3–K_2CO_3 and Li_2CO_3–K_2CO_3 immobilized on lithium aluminate towards the oxidative dimerization of methane was investigated at 750, 800, and 850°C. CH_4 conversion of 15–16%, C_2 yield of 9–10%, and C_2 selectivity of 58–62% was obtained at 800°C. Catalytic activity increased with temperature and melt decarbonation, which can be correlated with a stabilization of peroxide species. Comparison between these melts and with Li_2CO_3–Na_2CO_3 shows that a higher amount of C_2 hydrocarbons, formed per second and per gram of carbonate, was obtained in Li_2CO_3–K_2CO_3. © 1995 Academic Press, Inc.

INTRODUCTION

The oxidative conversion of methane to more valuable chemicals or fuels, intensively investigated for more than 10 years, is still a very attractive field of research, as has been recently outlined by Krylov in his extensive review on this subject (1). In the last five years alkali molten carbonates have been investigated as candidate catalysts or additives to other catalysts for the oxidative transformation of methane into C_2 hydrocarbons (2–8). Belyaev *et al.* (9) even used a molten carbonate fuel cell reactor for the same purpose.

In previous work we have shown that the catalytic activity of bulk molten salts such as $Ba(OH)_2$ and molten carbonate is correlated with the presence of peroxide species in these melts (7, 10). This is in accordance with recent spectroscopic studies, where peroxide species, believed to be responsible for the activation of methane, have been detected on solid catalysts such as Ba/MgO and Ba/La_2O_3 (11, 12). A rather poor gas–liquid contact led us to use a solid support, γ-$LiAlO_2$, to immobilize the carbonate melt and enhance its catalytic performance. Promising results have been obtained in Li_2CO_3-Na_2CO_3 (C_2 yields of about 9.5% at 750°C), showing that, although $LiAlO_2$ support combined with an alumina reactor has a catalytic effect, the main activity of molten carbonate/support can be largely attributed to the molten phase (8). Other melts with similar properties, such as Na_2CO_3–K_2CO_3 and Li_2CO_3–K_2CO_3, should also have an interesting catalytic behaviour (13–15). A brief comparison of the thermodynamic properties of these eutectics follows below.

The decomposition of molten carbonate (i.e., in Na_2CO_3–K_2CO_3: $Na_2CO_{3\,\text{liquid}} \Leftrightarrow Na_2O_{\text{solid}} + CO_{2\,\text{gas}}$) and the oxoacidity definition in these melts were fully described elsewhere (7, 8). A comparison of the extent of the oxoacidity range $pK^*d = -\log K^*d$ (K^*d: autodissociation equilibrium constant), for Li–Na, Li–K, and Na–K carbonate eutectics, shows that their stability increases with alkali cation radius. pK^*d of Li–K, Li–Na, and Na–K are 3.87, 3.89, and 9.09, respectively at 750°C (15). This indicates that Na–K is much more stable than Li–Na and Li–K which have nearly the same stability. Determination of the oxidizing power of oxygen species is a fundamental parameter in catalytic oxidation reactions. Oxidation of M_2CO_3 yields O_2, O_2^- or O_2^{2-} species:

$$2M_2CO_3 - 4e^- \Leftrightarrow O_2 + 2CO_2 + 4M^+ \qquad [1]$$

$$2M_2CO_3 - 3e^- \Leftrightarrow MO_2 + 2CO_2 + 3M^+ \qquad [2]$$

$$2M_2CO_3 - 2e^- \Leftrightarrow M_2O_2 + 2CO_2 + 2M^+ \qquad [3]$$

The stability of these species is a function of the oxoacidity level and can be predicted from the variation of equilibrium potentials of systems (1), (2), and (3) vs oxoacidity characterized by $-\log P(CO_2)$. Figure 1 shows the evolution of these potentials (calculated from thermodynamic data (16) with respect to the O_2/M_2O reference system (15)) at 750°C, under practical conditions close to those used in the catalytic dimerization of methane: $P(O_2) = 6 \times 10^{-2}$ atm and activities of peroxide and superoxide species of 10^{-3}. The broken lines fix the limits between the corresponding carbonate melt and its oxidized forms O_2, O_2^- (dissociated form of MO_2) and O_2^{2-} (dissociated form of M_2O_2). These diagrams show that for

---

[1] To whom correspondence should be addressed.

0021-9517/95 $6.00

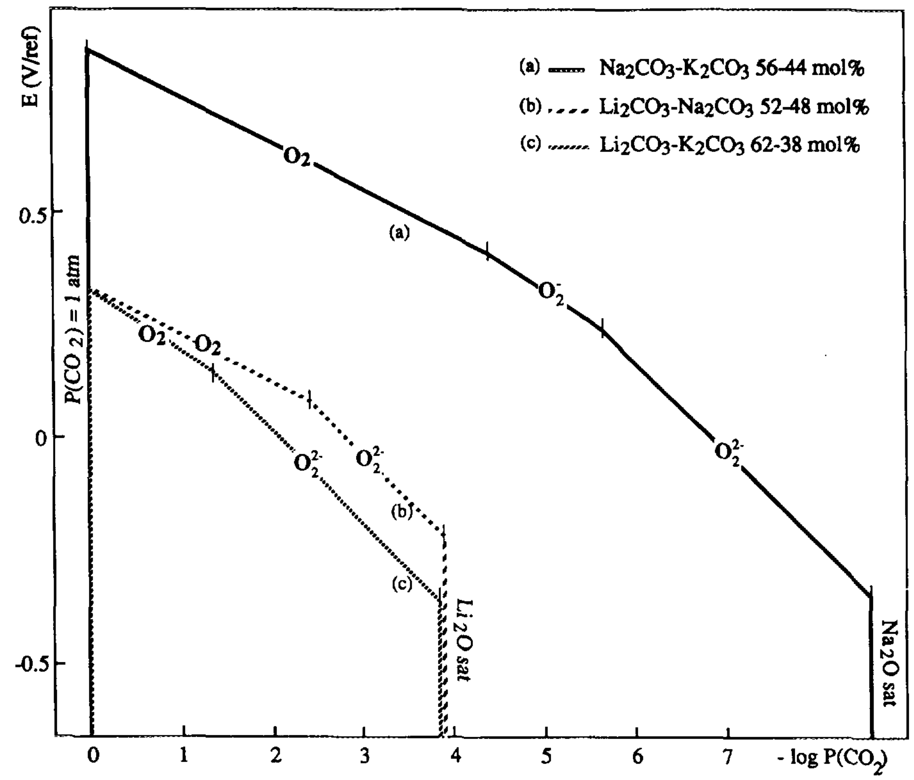

FIG. 1. Potential oxoacidity diagrams at 750°C of molten (a) Na_2CO_3–K_2CO_3, (b) Li_2CO_3–Na_2CO_3, and (c) Li_2CO_3–K_2CO_3, calculated from the Janaf Thermochemical Tables (13) under the following conditions: $P(O_2) = 6 \times 10^{-2}$ atm (1 atm = 1.013×10^5 Pa) and $a(O_2^{2-}) = a(O_2^-) = 10^{-3}$. Ref. O_2/M_2O system (M = Li for Li–Na and Li–K; M = Na for Na–K (15).

the three mentioned eutectics the stable forms of oxidized M_2CO_3 are oxygen in oxoacidic media (high $P(CO_2)$ values) and peroxide species (M_2O_2) in oxobasic media (low $P(CO_2)$ values). Although peroxide species are stable in oxobasic levels in the three melts, their stabilization is easier (partial pressures of CO_2 easier to fix and to measure) in Li–K ($P(CO_2)$ up to $10^{-1.35}$ atm) and Li–Na ($P(CO_2)$ up to $10^{-2.4}$ atm) than in Na–K ($P(CO_2)$ up to $10^{-5.65}$ atm.). Therefore, it can be predicted that Li-containing carbonate eutectics should have the best catalytic performance towards methane dimerization, but that Na–K, because of its higher stability, should deteriorate less during catalytic operations.

In this work the behaviour of Na–K and Li–K eutectics at different temperature and oxoacidity levels was investigated, correlated with the stability of peroxide species and compared with Li-Na melt. Scanning electron microscopy combined with X-ray probe microanalysis was used to analyze the supported materials before and after catalytic reactions. The aim of this study was not only to test new materials among the many which already exist for the oxidative conversion of methane, but principally to understand the catalytic mechanisms in promising media such as supported molten carbonate.

METHODS

Na_2CO_3–K_2CO_3 (56–44 mol%) Li_2CO_3–K_2CO_3 (62–38 mol%) and Li_2CO_3–Na_2CO_3 (52–48 mol%) eutectics were mixtures of Merck reagents of analytical grade. Synthesis and characterization of γ-$LiAlO_2$ pellets were fully described in a previous paper (8).

Immobilization of molten eutectics within lithium aluminate support (porosity of 30–37%), set on a Ni disc carrier not wetted by the melt, was carried out during 24 h in an alumina reactor under a 80% CO_2–20% H_2O atmosphere. The selected temperature was slightly higher than that corresponding to the melt fusion: 750°C (Na–K) or 520°C (Li–K and Li–Na).

The catalytic reactor and gas chromatograph system were described elsewhere (8).

Scanning Electron Microscopy

The morphology of samples was analyzed by SEM associated with X-ray probe microanalysis (JEOL T330A). SEM micrographs of pure $LiAlO_2$, as described previously (8), showed a regular structure formed by particles

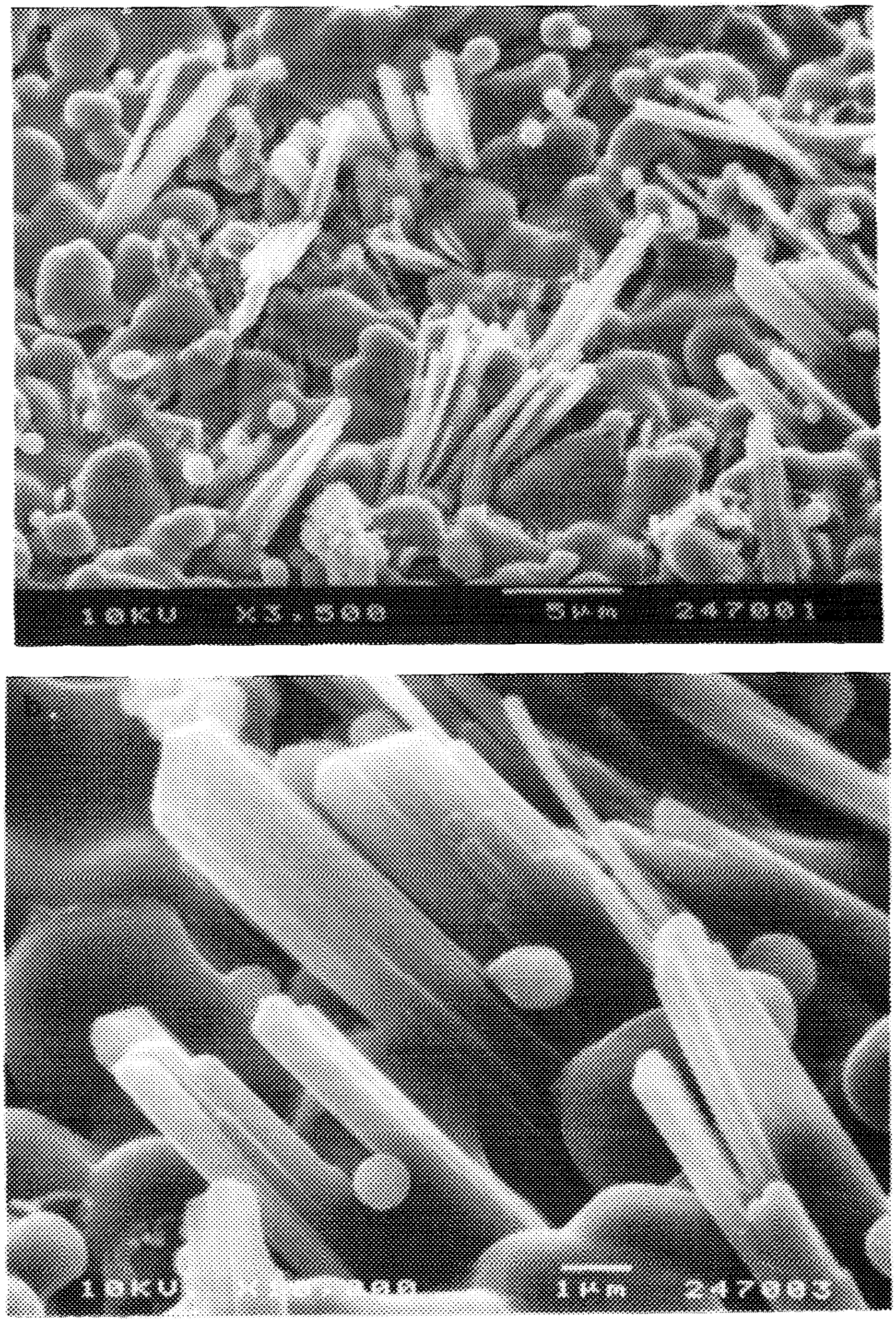

FIG. 2. SEM micrographs of Na_2CO_3–K_2CO_3/$LiAlO_2$: 12.9 wt%, after catalytic reaction: 270 h at 750–850°C under the reactant gas mixture (initial pressures of 138.5 Torr CH_4, 47.0 Torr O_2, 574.5 Torr He, total flow rate of 58.2 ml/min) or CO_2 at atmospheric pressure. (a) enlargement ×3500 (b) enlargement ×10,000.

of size 0.1 to 0.5 μm. The same structure was observed for Li_2CO_3–Na_2CO_3/$LiAlO_2$, Li_2CO_3–K_2CO_3/$LiAlO_2$ and Na_2CO_3–K_2CO_3/$LiAlO_2$ before catalytic reaction. X-ray probe microanalysis shows that carbonate eutectics form a thin layer at the surface of the lithium aluminate particles (about 200 μm in the case of Li–Na, as previously determined (8)). After extended catalytic reaction (282 h for Li–Na, 270 h for Na–K and 100 h for Li–K), samples presented a microstructural change, as shown in Figs. 2 and 3. Particles coalesced into aggregates from 0.5 to 5 μm in size in the case of Li–K and Na–K (2 to 10 μm in the case of Li–Na), which reduced significantly the con-

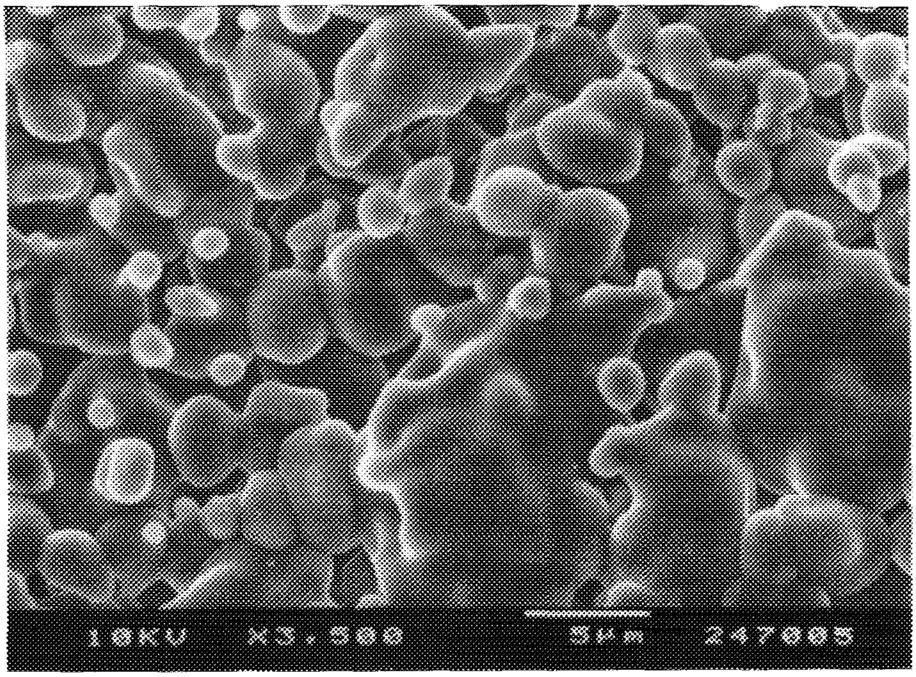

FIG. 3. SEM micrograph of Li_2CO_3–K_2CO_3/$LiAlO_2$: 14.9 wt%, after catalytic reaction: 100 h at 750–850°C under the reactant gas mixture (initial pressures of 138.5 Torr CH_4, 47.0 Torr O_2, 574.5 Torr He, total flow rate of 58.2 ml/min) or CO_2 at atmospheric pressure.

tact area between the supported carbonates and the reactants. Numerous whiskers (thickness of about 0.3 and 0.5 μm and length of about 5 to 10 μm) were observed, as clearly shown in Fig. 3b. Elemental analysis showed the presence of Na in Li–Na and Na–K melts and K in Na–K and Li–K melts, as indicated in Table 1. These whiskers, according to the melt concerned, are supposed to be formed either by sodium (or potassium) carbonate or by sodium or potassium oxide. Lithium cannot be detected by X-ray probe microanalysis.

RESULTS AND DISCUSSION

Table 2 shows the influence of the oxoacidity on the catalytic performance of molten Na_2CO_3–K_2CO_3 (12.9 wt% eutectic content/$LiAlO_2$) at 800°C and 850°C, re-

TABLE 1

Elemental Analysis of the Supported Carbonate Samples by X-Ray Probe Microanalysis

Sample	Area of analysis (μm^2)	Energy of primary electrons (keV)	View	Detected peaks[a] Al	Na	K
$LiAlO_2$ only	500	10	global	+++		
Li–Na 10.2% before catalysis	1.25	10	particles	+++	–	
	1.25	5	particles	+++	+	
Li–Na 10.2% after catalysis	500	5	global	+++	+	
	2.25	5	particles	+++	–	
	2.25	5	whiskers	+++	++	
Li–Na 16.7% after catalysis	500	10	global	+++	+	
	55	10	whiskers	+++	+++	
Na–K after catalysis	800	10	global	+++	+	+
	4	10	particles	+++	–	–
	4	10	whiskers	++	+++	+
Li–K after catalysis	800	10	global	+++		+
	4	10	coalescence area	+++		++

[a] +++ high intensity peak, ++ medium intensity peak, + low intensity peak, – no peak detected.

TABLE 2

Influence of the Acidity on the Oxidative Dimerization of Methane in Na_2CO_3–K_2CO_3 at 800 and 850°C

		Selectivity (%)				Conversion (%)			
Assay	*t* (h)	CO_2	CO	C_2H_4	C_2H_6	O_2	CH_4	C_2 selectivity (%)	C_2 yield (%)
				(a) 800°C					
1	23	41.0	2.3	25.4	31.4	48.5	14.2	56.7	8.0
2	95	37.8	2.6	28.5	31.1	53.6	15.1	59.6	9.0
CO_2 1 atm fixed during 10 h from 102 h to 112 h)									
3	119	39.4	2.7	27.3	30.7	50.9	14.4	58.0	8.4
4	143	40.4	2.5	26.0	31.1	46.5	13.1	57.1	7.5
5	167	41.0	2.8	25.7	30.5	47.3	13.6	56.2	7.6
6	191	39.5	2.5	27.2	30.9	51.2	15.8	58.1	9.2
7	262	38.7	2.6	27.8	30.8	51.2	15.4	58.6	9.0
				(b) 850°C					
1	28	41.4	5.5	32.6	20.5	78.3	20.6	53.1	10.9
2	100	38.8	5.4	34.0	21.6	77.3	21.1	55.8	11.8
CO_2 1 atm fixed during 10 h from 102 h to 112 h									
3	123	39.6	4.8	32.1	23.5	69.0	18.4	55.6	10.2
4	147	39.1	5.0	32.7	23.7	68.2	18.2	55.9	10.2
5	171	39.6	5.3	31.7	23.4	68.1	18.0	55.1	9.9
6	195	39.2	4.8	33.4	22.7	73.6	21.5	56.1	12.1
7	266	39.2	5.2	33.3	22.3	73.8	20.7	55.6	11.5

Note. General conditions: 5 mol% of Na_2CO_3–K_2CO_3 in 0.486 g of $LiAlO_2$; initial pressures of 138.5 Torr (1 Torr = 133.5 Pa) CH_4, 47.0 Torr O_2, 574.5 Torr He, total flow rate of 58.2 ml/min. *t* is the time during which the catalyst is maintained at 750°C under the reactant gas mixture (during the different assays), carbon dioxide at atmospheric pressure (during 10 h between assays 2 and 3) or helium at atmospheric pressure (between assays 1–2, 3–4, 4–5, 5–6, 6–7, and 7–8).

spectively. The melt becomes more oxoacidic when a known CO_2 pressure, higher than that corresponding to a "neutral" solution ($P(CO_2) = 10^{-4.2}$ atm at 800°C and $10^{-3.9}$ atm at 850°C), is set above the melt. On the contrary, the oxobasicity increases with the slow decarbonation of the melt occurring at high temperature (formation of oxide species). At 800°C, an increase in C_2 selectivity (56.7 to 59.6%) and C_2 yield (8.0 to 9.0%) was observed after heating the melt under helium during 72 h (Table 1a: from assay 1 to 2). The same situation occured at 850°C (Table 1b: assay 1 to 2). When CO_2 was placed over the melt, increasing the oxoacidity of the melt, the catalytic performance fell at both temperatures (about 1.5–2.0% in C_2 yield). This moderate oxoacidity effect was limited probably because of the low solubility of CO_2 (around 5×10^{-4} mol kg^{-1} at these temperatures (17)), which means that low amounts of O_2^{2-} were still present and active in the melt. When the reaction time increased, provoking an increase in the oxobasicity, C_2 yields became progressively higher (9.2 and 12.1%, respectively, at 800 and 850°C). In assays 7 (Table 1a and 1b, respectively), after a very long reaction time, C_2 yield values slightly fell, probably because of the formation of solid particles (presence of whiskers shown in Fig. 2b) of sodium oxide ($Na_2CO_3 \rightarrow Na_2O$) and potassium oxide ($K_2CO_3 \rightarrow K_2O$), as indicated in Table 1, making the contact between gas and molten salt more difficult. It should also be noted that oxygen and methane conversion increased with temperature, reaching values higher than 20% for methane and 70% for oxygen at 850°C.

In the case of Li_2CO_3–K_2CO_3 eutectic (14.9 wt% eutectic content/$LiAlO_2$), as shown in Table 3, oxygen conversion was about 10% higher at 800°C than in Na_2CO_3–K_2CO_3, whereas methane conversion, C_2 selectivity and C_2 yield had more similar values. The same oxoacidity effect was observed, for example at 800°C; C_2 yield fell

TABLE 3

Influence of the Acidity and Temperature on the Oxidative Dimerization of Methane in Li_2CO_3–K_2CO_3

		Selectivity (%)				Conversion (%)			
Assay	T (°C)	CO_2	CO	C_2H_4	C_2H_6	O_2	CH_4	C_2 selectivity (%)	C_2 yield (%)
1	700	48.9	1.9	16.3	32.9	37.0	10.4	49.2	5.1
2	750	38.8	1.7	24.6	34.9	47.4	12.3	59.5	7.3
3	800	36.6	2.3	31.0	30.1	62.8	15.8	61.1	9.7
CO_2 1 atm fixed during 60 h									
5	800	39.2	2.6	28.0	30.2	54.6	13.3	54.6	7.7

General conditions: 5 mol% of Li_2CO_3–K_2CO_3 in 0.486 g of $LiAlO_2$; initial pressures of 138.5 Torr CH_4, 47.0 Torr O_2, 574.5 Torr He, total flow rate of 58.2 ml/min.

from 9.7 to 7.7% and C_2 selectivity from 61.1 to 54.6% in the presence of CO_2.

In both eutectics considered, experimental evidence was obtained for the role of peroxide species, related to the oxobasicity of the melt, on catalytic performance. This is in agreement with the results obtained in Na_2CO_3–K_2CO_3 (7) without support and Li_2CO_3–Na_2CO_3/$LiAlO_2$ (8), as well as with the mechanism proposed by Ito *et al.* (18, 19) involving monoatomic peroxide ions O^- in the heterogeneous catalytic reaction of methane dimerization. O^-, supposed to be formed by the dissociation of O_2^{2-} at high temperature, reacts with methane yielding methyl radicals responsible for ethane and ethene formation. The controversial role of CO_2, which can also inhibit secondary reactions of methyl radicals with the solid catalyst according to Wang *et al.* (20), has been discussed in a previous paper (8). Lunsford *et al.* (11) also observed a "poisoning effect" of CO_2 with respect to the catalytic activity of Ba/MgO solid catalyst; they attributed it to a decrease of peroxide concentration by the following reaction: $\frac{1}{2}O_2^{2-} + CO_2 \rightarrow CO_3^{2-}$). In fact, the correlation between the activity of oxide catalysts and their basicity has been outlined by several authors (21–24).

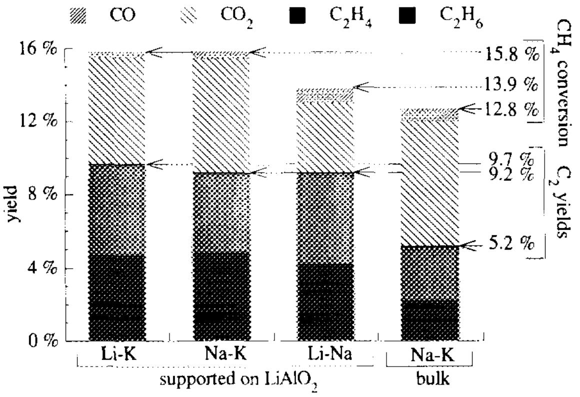

FIG. 4. Comparison of the catalytic performance of supported Li–K (14.9 wt%), Li–Na (10.2 wt%), Na–K (12.9 wt%), and the best results obtained in 150 g of bulk Na–K at 800°C.

Figure 4 shows the performance of the supported samples with respect to bulk Na–K at 800°C. Supported phases have the same behaviour, with slightly better results in the case of Li–K, but this can be due to the higher Li–K content/$LiAlO_2$ (14.9 wt%). CH_4 conversion is lower in the case of Li–Na which is in a smaller proportion with respect to the other melts (10.2 wt%). The effect of immobilization is clearly noted at 800°C when comparing, at the same flow rate and similar oxoacidity levels, the performance of supported Na–K/$LiAlO_2$: 12.9 wt% (C_2 yield 9.2%) with the best results obtained in 150 g bulk Na–K (C_2 yield 5.6%).[2]

In order to correlate catalytic activity with the nature and carbonate/$LiAlO_2$ content, as well as with its thermodynamic properties, we have determined the amount of C_2 products formed per second and per gram of supported carbonate (in nmoles s^{-1} g^{-1}). Figure 5 shows the variation of this amount with temperature. The same tendency can be noted in the case of Na–K and Li–Na. Li–K appears to be the best supported catalyst among the three carbonate eutectics, which is in accordance with the fact that peroxide species are thermodynamically sta-

---

[2] Flow rate and oxoacidity levels were optimized (4, 7).

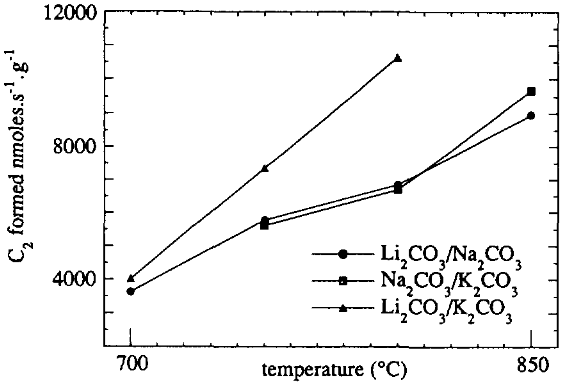

FIG. 5. Variation of the amount of C_2 products with the temperature in molten carbonate eutectics.

ble over a wider oxoacidity range, viz. $P(CO_2) \leq 10^{-1.35}$ atm, than in the other eutectics.

CONCLUSIONS

Na–K, Li–K, and Li–Na carbonate eutectics present an interesting catalytic activity towards methane dimerization, enhanced by their immobilization on a solid support, $LiAlO_2$, which allows a better contact between reactant gas and molten phase.

The catalytic performance of molten carbonate depends on the presence of peroxide species, which are stabilized in oxobasic media. Thus, as can be predicted thermodynamically, this activity increases with melt decarbonation and with increase of temperature (allowing formation of a larger quantity of peroxide ions from $O^{2-} + \frac{1}{2}O_2$).

Comparison between the three eutectics indicates that the amount of C_2 produced per second and per gram of supported carbonate is greater when Li–K catalyst is used, which corresponds to an easier stabilization of peroxide species in this melt. Nevertheless, in the best catalytic conditions (melts partially decarbonated), similar values of C_2 yield were obtained overall with the three catalysts.

After extended use of the supported catalysts, the catalytic activity falls. This can be correlated with a microstructural change of the samples: particles coalesce, showing the presence of whiskers partly formed by alkali oxide. A partial pressure of CO_2 above the melt (fixing the oxoacidity level), low enough to allow peroxide stabilization, could be a good solution to avoid the formation of alkali oxide and increase catalyst lifetime. These aspects require further investigation.

ACKNOWLEDGMENTS

Professor H. Wendt (Institut für Chemische Technologie, Darmstadt, Germany) is gratefully acknowledged for his constant interest and helpful advice and W. Rummel (Siemens, Germany) for his contribution in sample preparation. We also thank L. Robbiola for his contribution in SEM analysis.

REFERENCES

1. Krylov, O. V., *Catal. Today* **18,** 209 (1993).
2. Conway, S. J., Szanyi, J., and Lunsford, J. H., *Appl. Catal.* **56,** 149 (1989).
3. Geerts, J. W. M. H., van Kasteren, H. M. N., and van der Wiele, J., *J. Chem. Soc. Chem. Commun.* 802 (1990).
4. Moneuse, C., Doctorate thesis, ENSCP, Paris, 1990.
5. Dubois, J. L., and Cameron, C., *Chem. Lett.* 1089 (1991).
6. Noazki, T., and Fujimoto, K., *J. Chem. Soc. Chem. Commun.* 1248, (1992).
7. Moneuse, C., Cassir, M., Martin, G., and Devynck, J., *Appl. Catal.* **63,** 67 (1990).
8. Tashjian, V., Cassir, M., Devynck, J., and Rummel, W., *Appl. Catal.* **108,** 157 (1994).
9. Belyaev, V. D., Sobyanin, V. A., Parmon, V. N., Freni, S., and Aquino, M., *Catal. Lett.* **17,** 213 (1993).
10. Moneuse, C., Cassir, M., Piolet, C., and Devynck, J., *Appl. Catal.* **63,** 67 (1990).
11. Lunsford, J. H., Yang, X., Haller, K., Laane, J., Mestl, G., and Knözinger, H., *J. Phys. Chem.* **97,** 13810 (1993).
12. Yamashita, H., Machida, Y., and Tomita, A., *Appl. Catal.* **79,** 203 (1991).
13. Moutiers, G., Cassir, M., Piolet, C., and Devynck, J., *Electrochim. Acta* **36,** 1063 (1991).
14. Moutiers, G., Cassir, M., and Devynck, J., *J. Electroanal. Chem.* **324,** 175 (1992).
15. Cassir, M., Moutiers, G., and Devynck, J., *J. Electrochem. Soc.* **140,** 3114 (1993).
16. "Janaf Thermochemical Tables," 3rd ed., U.S. Department of Commerce, Washington, DC, 1986.
17. Appleby, A. J., and van Drunen, C., *J. Electrochem. Soc.* **127,** 1655 (1980).
18. Ito, I., and Lunsford, J. H., *Nature (London)* **314,** 721 (1985).
19. Ito, I., Wang, J. X., Lin, C. H., and Lunsford, J. H., *J. Phys. Chem. Soc.* **107,** 5062 (1985).
20. Wang, D., Xu, M., Shi, C., and Lunsford, J. H., *Catal. Lett.* 323 (1993).
21. Bytyn, W., and Baerns, M., *Appl. Catal.* **29,** 199 (1986).
22. Roos, J. A., Bakker, A. G., Bosch, H., van Ommen, J. G., and Ross, J. R. H., *Catal. Today* **1,** 133 (1987).
23. Agarwal, Y. K., Migone, R. A., and Marcelin, C., *J. Catal.* **121,** 110 (1990).
24. Maitra, A. M., Campbell, I., Tyler, R. J., *Appl. Catal.* **85,** 27 (1992).